Penerbit Akademia Baru

CFD Letters

Journal homepage: www.akademiabaru.com/cfdl.html
ISSN: 2180-1363

Effect of Blade Depth on the Energy Conversion Process in Crossflow Turbines

Open Access

Dendy Adanta[2], Warjito[1], Budiarso[1], Aji Putro Prakoso[1], Elang Pramudya Wijaya[1,*]

[1] Department of Mechanical Engineering, Faculty of Engineering, Universitas Indonesia, Depok 16424, West Java, Indonesia
[2] Department of Mechanical Engineering, Faculty of Engineering, Universitas Sriwijaya, Indralaya 30662, South Sumatera, Indonesia

ARTICLE INFO

Article history:
Received 22 November 2019
Received in revised form 18 January 2020
Accepted 23 January 2020
Available online 31 January 2020

Keywords:
pico hydro; crossflow turbine; blade depth; computation

ABSTRACT

In 2019, more than 4.5 million people in remote areas of Indonesia had limited access to electricity. To solve the electricity crisis in remote areas, pico-hydro-type crossflows are recommended for independent power plants. When designing a crossflow turbine, the blade depth is an important parameter. Crossflow turbine performance is affected by the nozzle and the blade. This study will discuss the effect of blade depth on the energy conversion process in crossflow turbines. Using computational methods, this study compares three blade depths: 1.5-mm, 3-mm and 4.5-mm. Two-dimensional transient simulations were carried out using the six degrees of freedom (6 DoF) approach. The viscous model was shear stress transport (SST) k-ω and 6 with the volume of fluid (VoF) approach. From the results, the maximum efficiency of crossflow turbines shows that blades with greater depths tend to have higher efficiency. However, the 3-mm blade depth showed maximum efficiency vulnerable to wider than 4.5-mm and 1.5-mm depths. Thus, the 3-mm blade depth is recommended for this condition.

1. Introduction

In 2019, more than 4.5 million people in Indonesia did not yet have access to the electricity grid [1]. Remote areas of Indonesia are experiencing an electricity crisis due to their hilly topography and islands, which make it difficult for electricity to reach them [2]. To solve the electricity crisis in remote areas, pico-hydro-type crossflows are recommended for independent power plants [3]. Indonesia has potential hydro-energy sources up to 19 GW with low-head (< 5 m) conditions [2]. Hydro energy extraction using hydropower with pico scales is a suitable solution for low-head conditions (< 5 m). This is because, for pico scales, the manufacturing process and maintenance are not complex compared to larger scales. These are the reasons why pico-hydro-type crossflows are suitable for independent power plants in remote areas in Indonesia [2, 4].

The pico-hydro-type crossflow is a power plant with capacity under 5 kW. It has several advantages, including long operational times, large potential resources and greater energy density, about 832 times greater than that of wind and solar power [5]. The pico-hydro-type crossflow is one

* *Corresponding author.*
E-mail address: elangpw@outlook.com (Elang Pramudya Wijaya)

of the turbines that is considered appropriate for power plants in remote areas [2, 4, 6-7] since the crossflow turbine can work in low-head (<5 m) conditions and high-discharge deviations [7].

The crossflow turbine is an impulse that converts the kinetic energy of water to rotate runners [4, 7]. When water hits the runner blades, it transfers its momentum to the blades [8]. The energy conversion of crossflow turbines occurs in two stages [9]: 68.5% of energy is transferred in the first stage, and 31.5% is transferred in the second stage.

To obtain a crossflow turbine's optimum performance, several design parameters, such as number of blades, blade shapes, nozzle shapes and guide vanes, must be considered. However, blade shape most significantly affects the performance of the crossflow turbine [7]. This is because the blade is where energy is converted from water to the turbine. Based on previous studies, blades with 3-mm blade depths have higher efficiency and are more stable than others [7]. However, the results of previous studies have not been validated, and the results are still disputed. Therefore, a review is needed to validate whether the blade depth significantly influences the energy conversion process in the crossflow turbine. Thus, this study will re-investigate blade depth and validate the results.

2. Methodology

2.1 Geometry of The Turbine

The geometry of this crossflow turbine uses [10] model turbines with various blade depths. Details of the geometry dimensions can be seen in Table 1.

Table 1
Turbine design parameters

Description	Dimension
Outer diameter, D_o	162.00 mm
Inner diameter, D_i	104.00 mm
Number of blades	35
Blade chord length, C	30.96 mm

A representation of Table 1 can be seen in Figure 1.

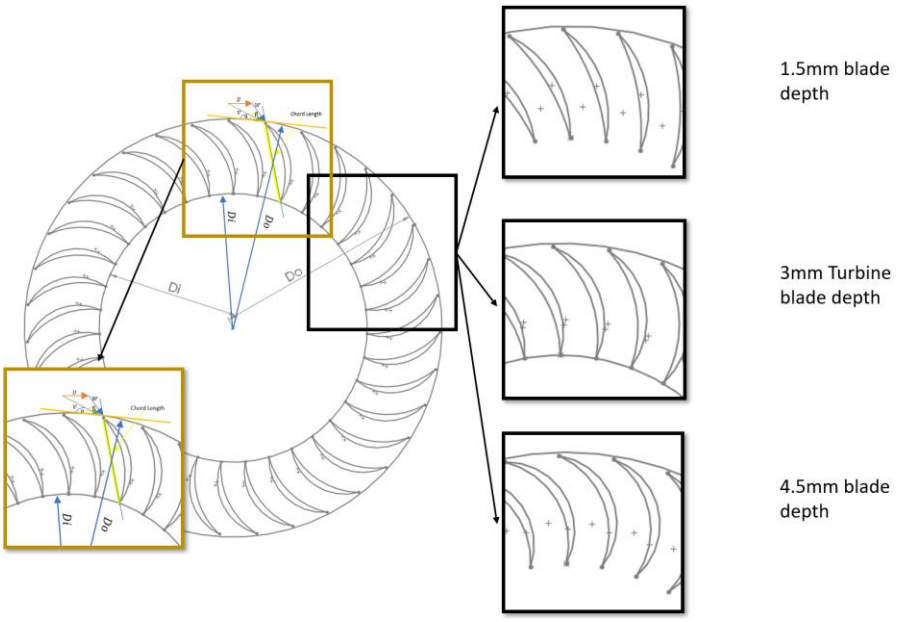

Fig. 1. 2D model of the blade

In this simulation, the blade chord was constant, with varied blade depths multiplied by 0.5 times and 1.5 times the crossflow turbine model [10].

2.2 Simulation Setup

The simulation is run using ANSYS™ FLUENT® 18.2 Academic version. Simulation boundary conditions can be seen in Figure 2. The simulation uses a pressure inlet because the conditions are incompressible. The gravitational acceleration is $9.81\ m/s^2$. Multiphase volume of fluid (VoF) with implicit volume fraction parameters and implicit body force was used, employing water for the primary phase and air for the second phase. The volume of water is 1 in the inlet, while the value of air is 0. The transport of VoF can be seen in Eq. (1).

$$\frac{1}{\rho_q}\left[\frac{\partial}{\partial t}\left(\alpha_q\rho_q\right)+\nabla\cdot\left(\alpha_q\rho_q\vec{v}_q\right)=S_{a_q}+\sum_{p=1}^{n}(\dot{m}_{pq}-\dot{m}_{qp})\right] \tag{1}$$

where, $\dot{m}_{pq}$ is the transfer of mass from phase p to phase q [11]. Phase p is water and phase q is air. The shear stress transport (SST) k-ω viscous model was used because, based on assessments, this model is optimally suited for this case [6]. The transport of SST k-ω can be seen in Eq. (2) for k and Eq. (3) for ω.

$$\frac{\partial(\rho k)}{\partial t}+\frac{\partial(\rho k u_i)}{\partial x_i}=\frac{\partial}{\partial x_j}\left(\Gamma_k\frac{\partial k}{\partial x_j}\right)+G_k-Y_k+S_k \tag{2}$$

$$\frac{\partial(\rho\omega)}{\partial t}+\frac{\partial(\rho\omega u_i)}{\partial x_i}=\frac{\partial}{\partial x_j}\left(\Gamma_\omega\frac{\partial\omega}{\partial x_j}\right)+G_\omega-Y_\omega+D_\omega+S_\omega \tag{3}$$

where G_k and G_ω are the generation of k and ω due to mean velocity gradient, respectively; Γ_k and Γ_ω are the effective diffusivity of k and ω, respectively; Y_k and Y_ω are the dissipation of k and ω due to turbulence, respectively; D_ω is a cross-diffusion term; S_k and S_ω are user-defined source terms.

The simulation uses a dynamic mesh approach with the six degrees of freedom (6 DoF) feature to better predict the fluid dynamics that occur in the crossflow turbine [4]. The 6 DoF feature requires some additional initial conditions, such as a moment of inertia and preload. This study used 1 N·m of preload, and the moment of inertia was determined by using computer-aided design software. In order to compute the translational motion of the turbine, the following equation was used:

$$\overrightarrow{v_g}=\frac{1}{m}\sum\vec{f}_G \tag{4}$$

where $\overrightarrow{v_g}$ is determined by Eq. (4). To determine the angular motion of the object, Eq. (5) was used:

$$\overrightarrow{\omega_B}=L^{-1}\left(\sum\overrightarrow{M_B}-\overrightarrow{\omega_B}\times L\overrightarrow{\omega_B}\right) \tag{5}$$

where L is the inertia, $\overrightarrow{M_B}$ is the moment vector of the blade, and $\overrightarrow{\omega_B}$ is the rigid body angular velocity. Both the angular and translational velocities were also used to find the position of the rigid body.

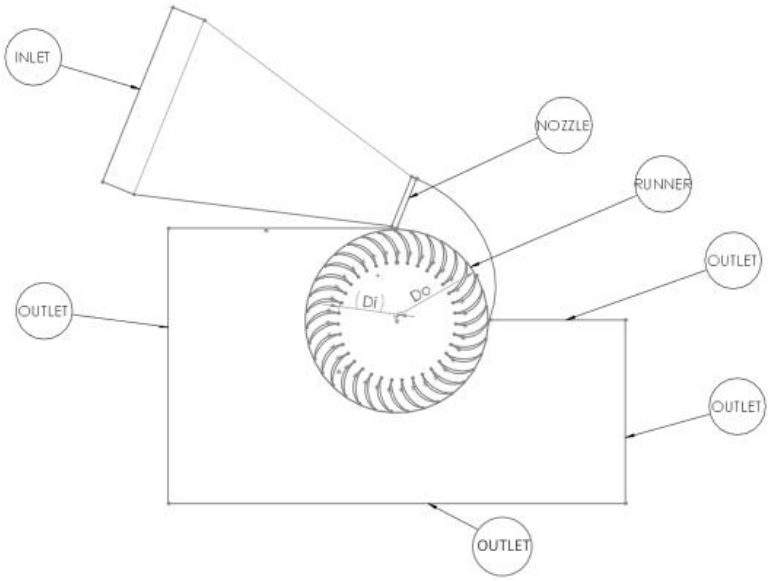

Fig. 2. Boundary condition

2.3 Mesh Independency Test

An accurate mesh was used to improve the quality of this simulation. Error was calculated from the Richardson extrapolation by using the grid convergence index (GCI), which was calculated based on Eq. (6).

$$GCI_{ab} = H\left|\frac{1}{\tau_a}\frac{\tau_b-\tau_a}{{r_{ab}}^K-1}\right| \times 100\% \tag{6}$$

where H is the safety factor of 1.25, K is the order of convergence observed, and r is the grid refinement ratio. r is represented in Eq. (7):

$$r_{ab} = \left(\frac{N_a}{N_b}\right)^{0.5} \tag{7}$$

where N is the mesh number. Further, the order of convergence observed (K) was determined using Eq. (8) by a numerical method [12-13]:

$$K_{n+1} = \frac{\ln\left(\left(\frac{\tau_c-\tau_b}{\tau_b-\tau_a}\left({r_{ab}}^K-1\right)\right)+{r_{ab}}^K\right)}{\ln(r_{ab}\cdot r_{bc})} \tag{8}$$

After all parameters were known, the exact torque (τ_{exact}) was determined. The exact torque or exact value is an approach to find out the true value when the number of mesh is infinity [14]. τ_{exact} can be determined using Eq. (9):

$$\tau_{exact} = \tau_a - \left(\frac{\tau_b-\tau_a}{{r_{ab}}^K-1}\right) \tag{9}$$

Several mesh independency tests were conducted using steady-state, single-phase methods.

3. Results

3.1 Independency Test Results

Four mesh sizes were estimated to find the suitable mesh size. Table 2 and Table 3 show the mesh independency test results and timestep independency test results, respectively. Several variations of mesh size started from 18k, 32k, 64k, 96k and 128k and were then translated to 1.99, 1.41, 1.15 and 1, respectively (normalised grid spacing) (see Table 2). Based on the GCI results, a mesh number of 96,649 elements was determined to be optimal to use with a GCI value of 1.47%. The visualisation of the mesh number of 96,649 elements can be seen in Figure 3.

With the GCI concept, the timestep value is also analysed to obtain the optimal timestep, called the timestep convergency index (TCI). Based on the analysis, this simulation used 0.0005 s of time with 5,000 timesteps, because the error is considered to be small at 1.35% (see Table 3).

Table 2
Mesh independency test results

Normalised Grid Spacing	Number of Elements	Torque [N·m]	GCI
1.99	32,484	255.06	-
1.41	64,450	266.59	1.54%
1.15	96,649	268.21	1.47%
1.00	128,848	269.84	0.99%
0.00	Infinite	271.98	-

Table 3
Timestep independency test results

Normalised Timestep Sizing	Timestep Size	Torque [N·m]	TCI
12.65	0.0032	109.82	-
	0.0008		
2.00		118.62	1.46%
1.58	0.0005	119.37	1.35%
1.00	0.0002	120.13	0.54%
0.00	0.0000	120.65	-

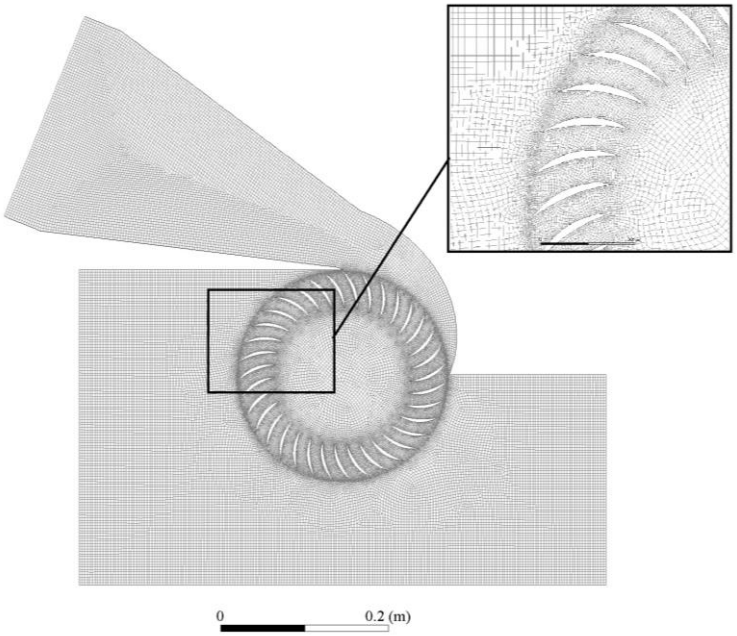

Fig. 3. 2D domain mesh visualisation: 96,435 elements

3.2 Crossflow Turbine Performance Results

Figure 4 demonstrates the computational results, which show the turbine velocity characterised by the ratio of rotation wheel velocity and absolute water velocity (U/V). According to the literature, the maximum efficiency of an impulse turbine occurs when the U/V ratio is between 0.42 and 0.50 [15]. In Figure 4(a), the maximum efficiency of the crossflow turbine occurs at a U/V ratio of 0.48 to 0.63, and blades with higher blade depth ratios tend to have higher efficiency.

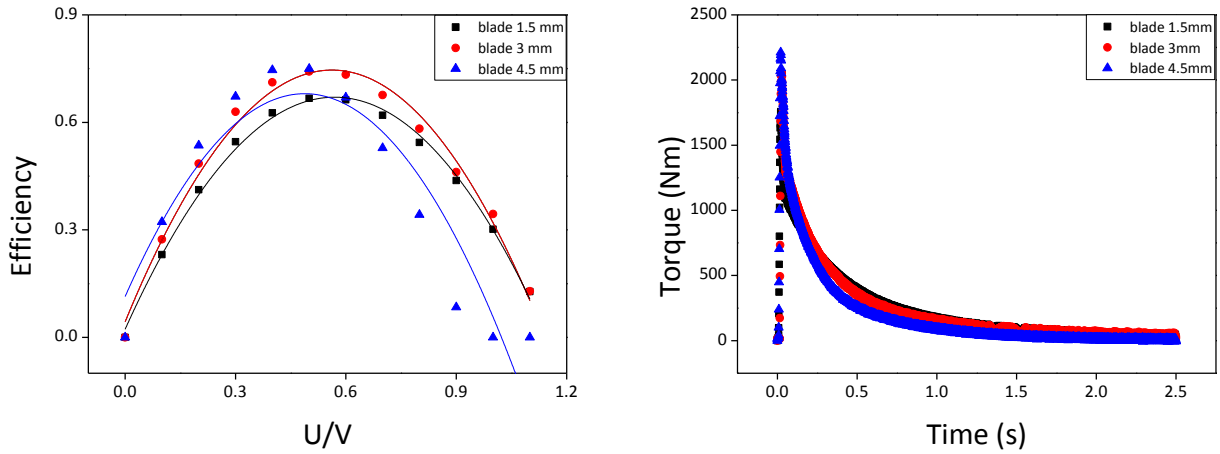

(a) Performance graph (b) Torque vs time

Fig. 4. The computational result

3.3 Discussion

The numerical simulation results obtained show that a blade depth of 3 mm has the highest efficiency. This result is convenient given the theoretical approach of crossflow blade curvature that is related to the water velocity angle and the runner's diameter ratio [16]. However, the higher impulse force impact in the first stage of energy transfer in this turbine, which resulted from increasing the blade depth, still could not increase this turbine's performance. The modification only disrupted the internal flow inside the crossflow turbine and reduced the energy transfer quality in the second stage. Figure 5 shows the total pressure contour at maximum efficiency condition. The total pressure contour of a blade depth of 4.5 mm in Figure 5(c) illustrates this situation.

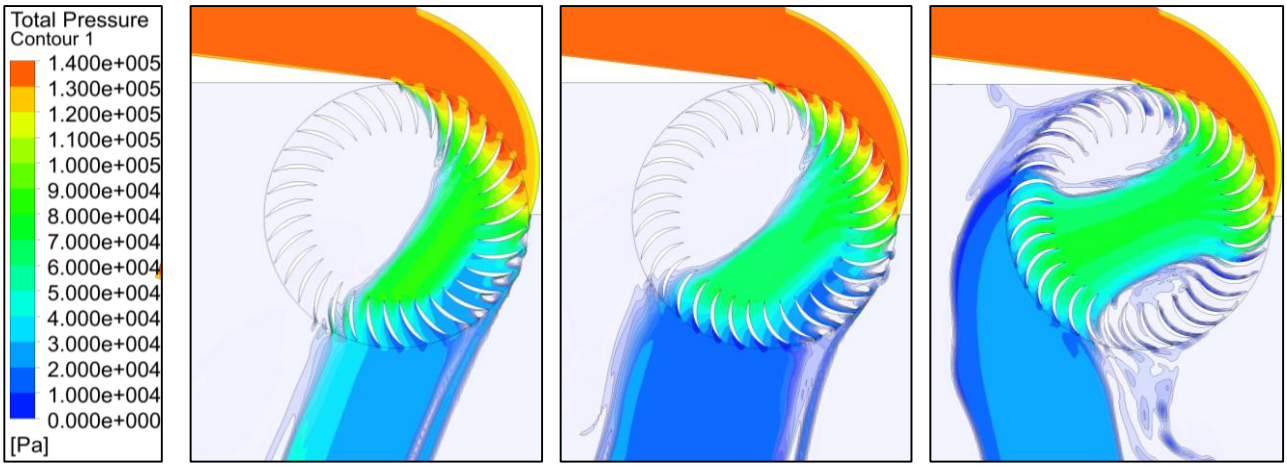

(a) Blade depth of 1.5 mm (b) Blade depth of 3 mm (c) Blade depth of 4.5 mm

Fig. 5. Total pressure contour at maximum efficiency condition

Total pressure of water is a variable that can represent the energy contained by water. In Figure 5, the energy transfer process in the first stage shows that the increased effect of impulse forces does not increase energy absorbed in the first stage. However, the difference in energy absorbed by the blade at each blade depth (see Figure 4(a)) due to the decreases in the total pressure drop in the second stage is different. Therefore, it is indicated that the blade depth variation affects the quantity of energy absorbed in the second stage.

The total pressure drops at the second stage for a blade depth of 1.5 mm (see Figure 5(a)) is about 40 kPa. On the other hand, for blade depths of 3 mm and 4.5 mm, there is a total pressure drop of about 65 kPa and 60 kPa, respectively. The obtained results in Figure 5 are suitable with the efficiency curve in Figure 4(a).

The difference in blade depth affects the turbulence condition at the internal flow of the crossflow turbine. Corresponding to prior studies by Adanta [4], [6] and Warjito [17], the imperfect design of the turbine blade could affect the throughflow. The effect of blade depth on throughflow is represented by the turbulence intensity contour in Figure 6.

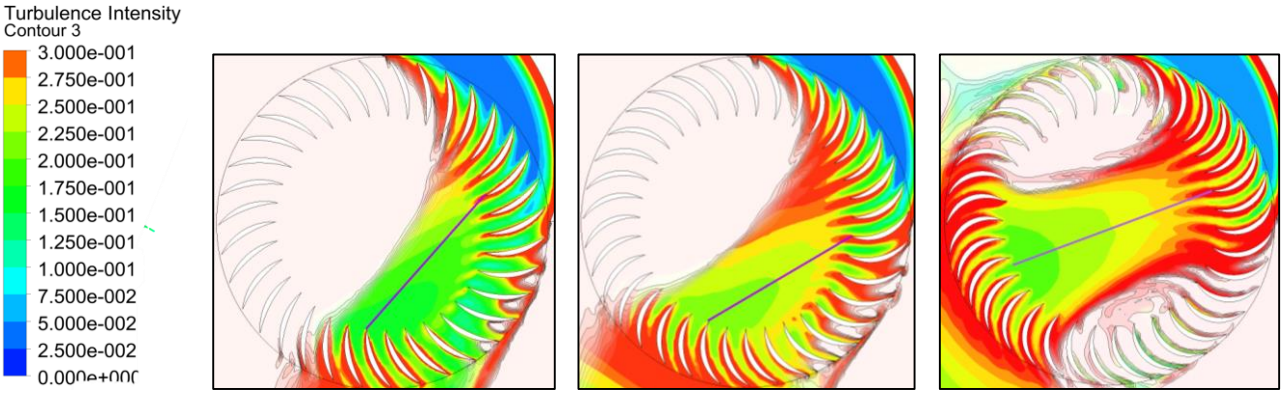

(a) Blade depth of 5 mm (b) Blade depth of 3 mm (c) Blade depth of 4.5 mm

Fig. 6. Turbulence intensity contour at throughflow

Figure 6 shows that greater blade depths result in higher turbulence intensity at the throughflow of the crossflow turbine. The quantification of turbulence intensity is shown in the purple line in Figure 6. Figure 7 demonstrates the turbulence intensity data contained in the purple line. From Figure 7, the turbulence intensity of water near the blade at the first stage is very high, especially for the 4.5-mm blade depth. The turbulence intensity for the 4.5-mm blade depth is very high, approaching 0.5. The high turbulence intensity for the 4.5-mm blade depth resulted from increased water inertia due to water passing through a curved path (the blade). This indicates that water energy is also needed for the mixing process, so that the quantity of energy possessed by the water is reduced. On the other hand, the turbulence intensity for the 1.5-mm blade depth is low both on the graphic and the contour results, which indicates smaller energy loss. However, for the 1.5-mm blade depth, the kinetic energy of the water is not completely absorbed by the blade, so the efficiency is low.

The result of this is that the 3-mm-depth blade crossflow turbine provides a more balanced approach to energy transfer quality and protection from energy loss inside the water caused by turbulence. Although the turbulence loss effect is very low, it still impacts the performance of the crossflow turbine, as happened with the 4.5-mm blade depth.

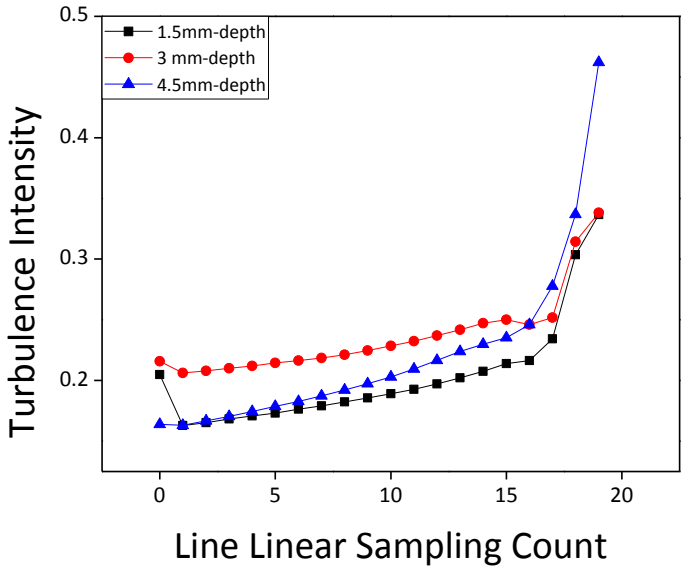

Fig. 7. Turbulence intensity graph on purple line for each case

4. Conclusions

The results of this study showed that higher blade depth ratios tend to have higher efficiency. The 4.5-mm blade depth design produced the highest efficiency, valued at 74.97%. However, the 3-mm blade depth had maximum efficiency vulnerable to depths wider than 4.5 mm and 1.5 mm. Thus, the 3-mm blade depth is recommended for this condition.

Acknowledgement

This work supported by the the Ministry of Research, Technology and Higher Education (KEMENRISTEK DIKTI) of the Republic of Indonesia with grant No: NKB-1853/UN2.R3.1/HKP.05.00/2019.

References

[1] KESDM. “Rasio Elektrifikasi.” 2019.
[2] Adanta, Dendy, Warjito Budiarso, and Ahmad Indra Siswantara. "Assessment of turbulence modelling for numerical simulations into pico hydro turbine." *Journal of Advanced Research in Fluid Mechanics and Thermal Sciences* 46, no. 1 (2018): 21-31.
[3] Ho-Yan, Bryan. “Design of a Low Head Pico Hydro Turbine for Rural Electrification in Cameroon.” PhD diss., University of Guelph, 2012.
[4] Adanta, Dendy, Warjito Budiarso, Ahmad Indra Siswantara, and Aji Putro Prakoso. "Performance comparison of NACA 6509 and 6712 on pico hydro type cross-flow turbine by numerical method." *Journal of Advanced Research in Fluid Mechanics and Thermal Sciences* 45, no. 1 (2018): 116-127.
[5] Sipahutar, Riman, Siti Masreah Bernas, and Momon Sodik Imanuddin. "Renewable energy and hydropower utilization tendency worldwide." *Renewable and Sustainable Energy Reviews* 17 (2013): 213-215.
[6] Siswantara, Ahmad Indra, Aji Putro Prakoso Budiarso, Gun Gun R. Gunadi, and Dendy Warjito. "Assessment of Turbulence Model for Cross-Flow Pico Hydro Turbine Numerical Simulation." *CFD Letters* 10, no. 2 (2018): 38-48.
[7] Adanta, Dendy, Richiditya Hindami, and Ahmad Indra Siswantara. "Blade Depth Investigation on Cross-flow Turbine by Numerical Method." In *2018 4th International Conference on Science and Technology (ICST)*, pp. 1-6. IEEE, 2018.
[8] Paish, Oliver. "Small hydro power: technology and current status." *Renewable and sustainable energy reviews* 6, no. 6 (2002): 537-556.
[9] De Andrade, Jesús, Christian Curiel, Frank Kenyery, Orlando Aguillón, Auristela Vásquez, and Miguel Asuaje. "Numerical investigation of the internal flow in a Banki turbine." *International Journal of Rotating Machinery* 2011 (2011): 1-12.
[10] Sammartano, Vincenzo, Gabriele Morreale, Marco Sinagra, and Tullio Tucciarelli. "Numerical and experimental

investigation of a cross-flow water turbine." *Journal of Hydraulic Research* 54, no. 3 (2016): 321-331.
[11] Fluent, A. N. S. Y. S. "ANSYS fluent theory guide 15.0." *Inc, Canonsburg, PA* (2013).
[12] Ali, Mohamed Sukri Mat, Con J. Doolan, and Vincent Wheatley. "Grid convergence study for a two-dimensional simulation of flow around a square cylinder at a low Reynolds number." In *Seventh International Conference on CFD in The Minerals and Process Industries (ed. PJ Witt & MP Schwarz)*, pp. 1-6. 2009.
[13] Xing, Tao, and Fred Stern. *Factors of safety for Richardson extrapolation for industrial applications*. No. IIHR-TR-466. IOWA UNIV IOWA CITY IIHR-HYDROSCIENCE AND ENGINEERING, 2008.
[14] Roache, Patrick J. "Quantification of uncertainty in computational fluid dynamics." *Annual review of fluid Mechanics* 29, no. 1 (1997): 123-160.
[15] Harinaldi, Budiarso. "Sistem Fluida Prinsip Dasar dan penerapan Mesin Fluida, Sistem Hidrolik, dan Sistem Penumatik." *Jakarta: Erlangga* (2015).
[16] Sammartano, Vincenzo, Costanza Aricò, Armando Carravetta, Oreste Fecarotta, and Tullio Tucciarelli. "Banki-Michell optimal design by computational fluid dynamics testing and hydrodynamic analysis." *Energies* 6, no. 5 (2013): 2362-2385.
[17] Warjito, Ahmad Indra Siswantara, Dendy Adanta, Aji Putro Prakoso, and Reza Dianofitra. "Comparison Between Airfoil Profiled Blade and Ordinary Blade in Cross-Flow Turbine Using Numerical Simulation." In *15th International Conference on Quality in Research*. 2017.